Supplemental Figures and Tables

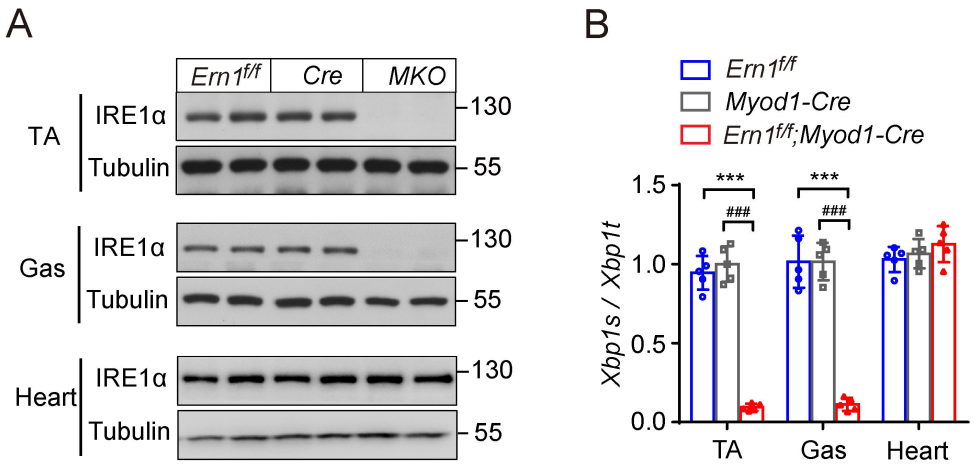

Supplemental Figure 1. Generation of skeletal muscle-specific IRE1α knockout mice. *Ern1*$^{f/f}$ and *Myod1-Cre* mice were utilized for intercrossing to produce *Ern1*$^{f/f}$*;Myod1-Cre* (*MKO*) mice. **(A)** Representative immunoblot analysis of IRE1α protein from Tibialis anterior (TA) and gastrocnemius (Gas) muscle as well as the heart of *Ern1*$^{f/f}$, *Myod1-Cre* and *Ern1*$^{f/f}$*;Myod1-Cre* mice (n = 5 mice per genotype). **(B)** Quantitative RT-PCR analysis of *Xbp1* mRNA splicing (n = 5 mice per genotype). $^{***}P<0.001$ relative to *Ern1*$^{f/f}$, and $^{###}P< 0.001$ relative to *Myod1-cre* by 1-way ANOVA with Bonferroni's multiple comparisons test.

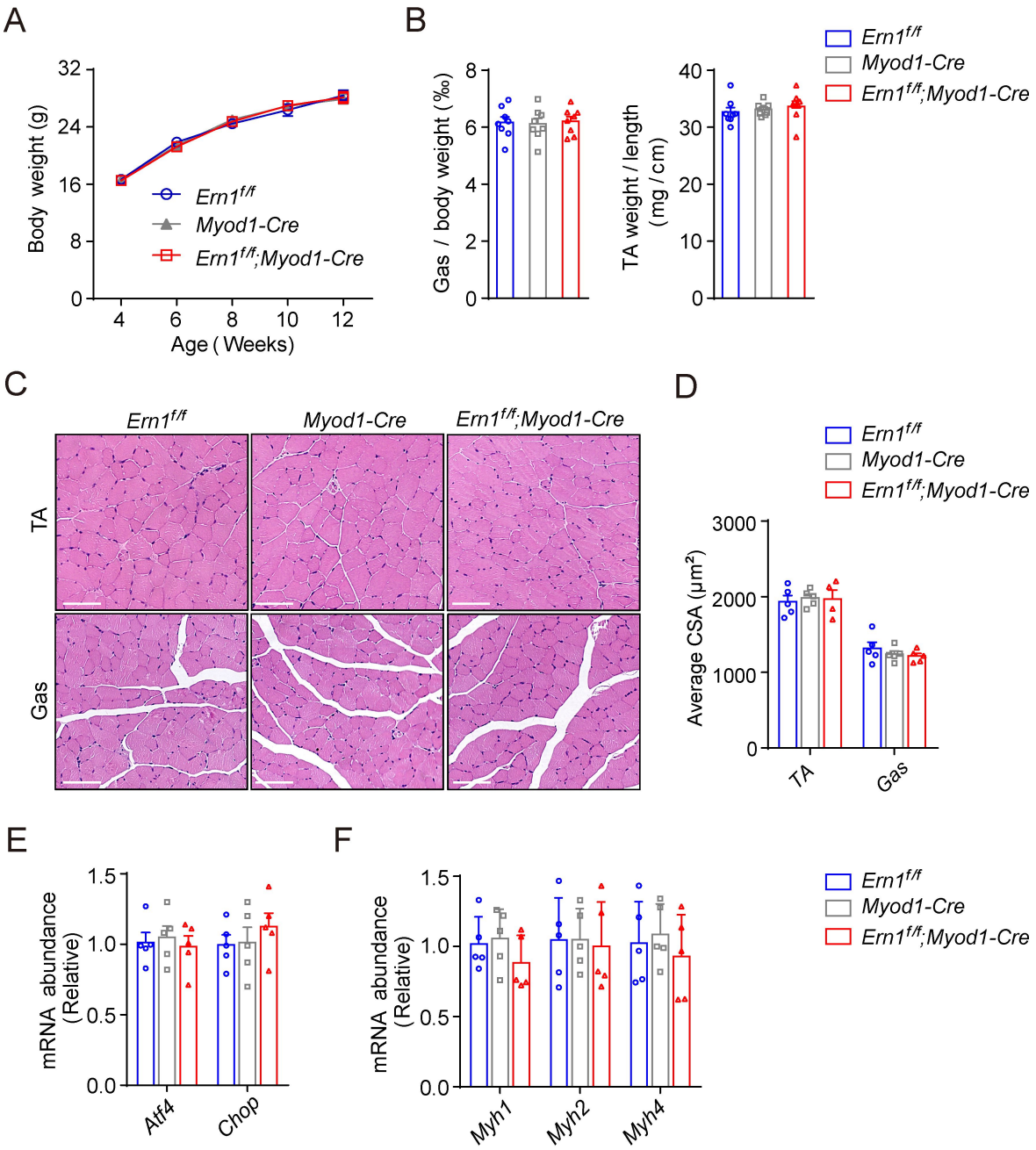

Supplemental Figure 2. Muscle IRE1α deficiency did not affect skeletal muscle development. (A) Body weight of male *Ern1*$^{f/f}$, *Myod1-Cre* and *Ern1*$^{f/f}$*;Myod1-Cre* mice at the indicated ages (n = 8 mice per genotype). **(B)** Gas muscle weight relative to body weight and TA muscle weight relative to tibia length from mice at 10 weeks of age (n = 8 mice per genotype). **(C)** Representative H&E staining of TA and Gas muscles (Scale bar: 100 μm), and **(D)** averaged myofibers cross-sectional areas (CSA) were measured in mice at 10 weeks of age (n = 5 mice per genotype). **(E, F)** Quantitative RT-PCR analysis of the mRNA abundance of **(E)** *Atf4* and *Chop* and **(F)** *Myh1*, *Myh2* and *Myh4* in TA muscles. Shown are results after normalization to *Gapdh* as the internal control (n = 5 mice per genotype). Significance was analyzed by 1-way ANOVA with Bonferroni's multiple comparisons test.

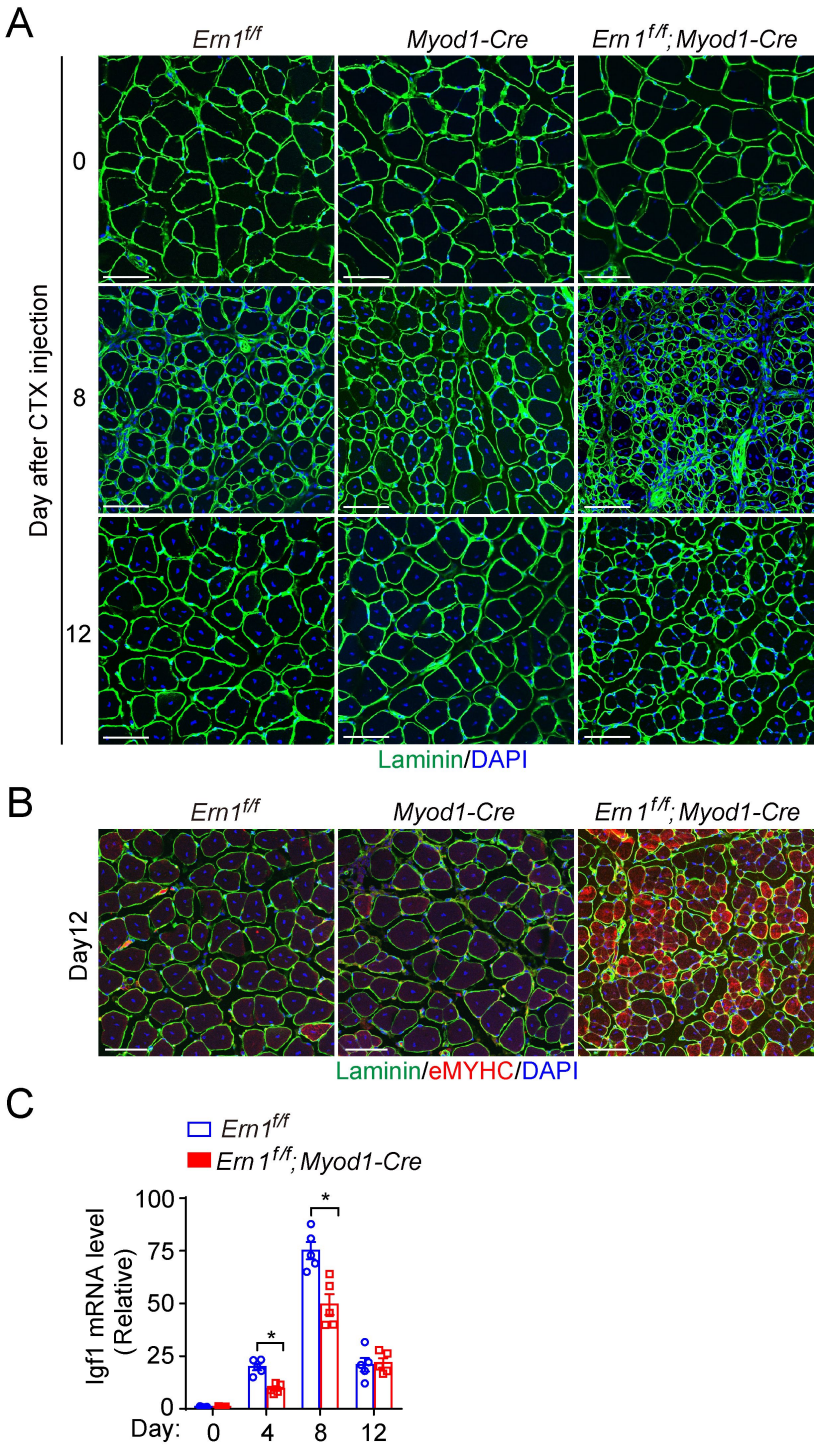

Supplemental Figure 3. Loss of muscle IRE1α impairs acute injury-induced skeletal muscle regeneration. (A) Representative Laminin staining of TA muscles from mice of the indicated genotype at 0, 8 or 12 days after CTX injection (n = 5 mice per group). **(B)** Representative immunostaining of Laminin (green) and eMyHC (Red) in TA muscles from mice of the indicated genotype at 12 days after CTX injection (n = 5 mice per group). Scale bars: 50 μm. **(C)** Quantitative RT-PCR analysis of *Igf1* mRNA abundance in TA muscles at the indicated time following CTX injuries (n = 5 mice per group). $^{*}P<0.05$ by 2-way ANOVA with Bonferroni's multiple comparisons test.

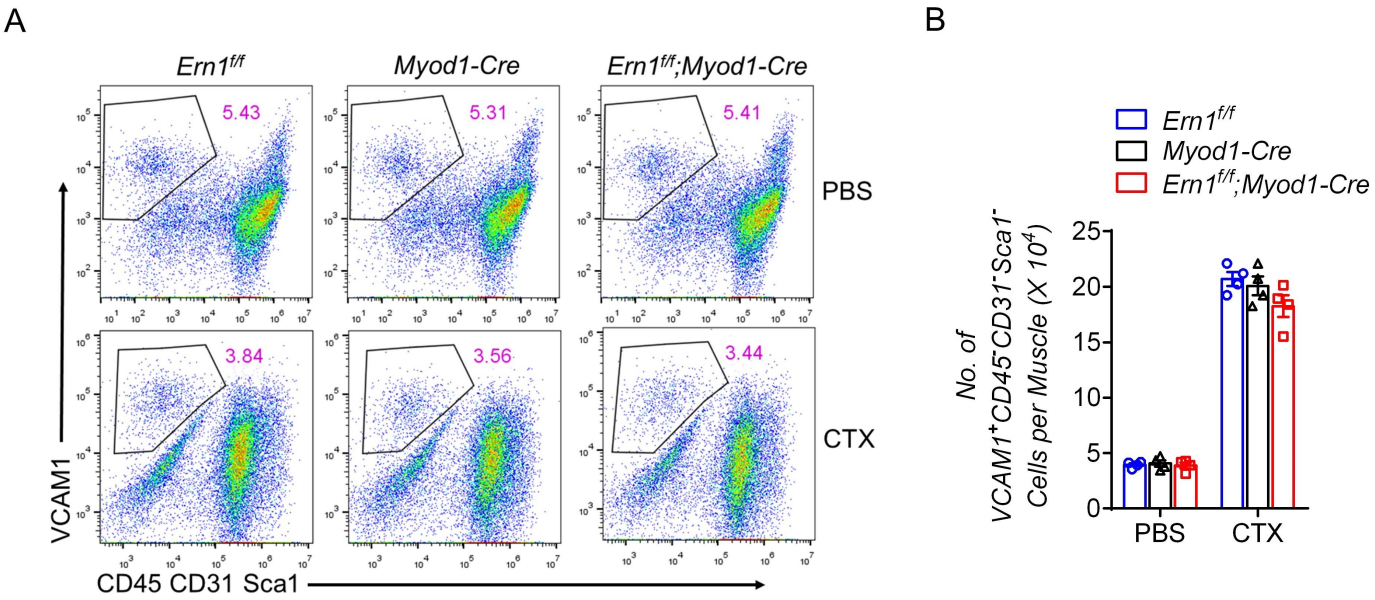

Supplemental Figure 4. IRE1α deficiency does not affect the abundance of MuSCs in response to acute muscle injury. Flow-cytometry analysis of MuSCs isolated from TA muscles of the indicated genotype at 3 days after PBS or CTX injection (n = 4 mice per group). (A) Representative FACS diagrams showing the expression of the indicated cell markers from sorted muscle cells. The percentages of $VCAM1^+CD45^-CD31^-Sca1^-$ cells are indicated. **(B)** Amounts of $VCAM1^+CD45^-CD31^-Sca1^-$ cells from each group. Significance was analyzed by 2-way ANOVA with Bonferroni's multiple comparisons test.

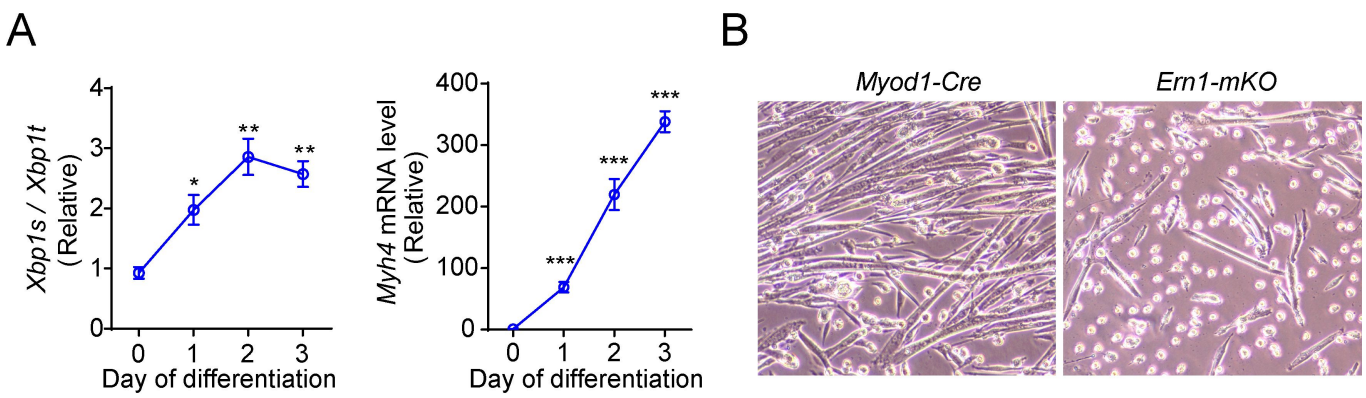

Supplemental Figure 5. IRE1α regulates myoblast differentiation. (A) Primary myoblasts were isolated from TA muscle and differentiated for up to 3 days into myotubes. Quantitative RT-PCR analysis of *Xbp1* mRNA splicing and the abundance of *Myh4* mRNA. Data are presented as the mean ± SEM (n = 3 independent experiments). $^{*}P < 0.05$, $^{**}P < 0.01$, $^{***}P < 0.001$ relative to day 0 by 1-way ANOVA with Bonferroni's multiple comparisons test. **(B)** TA myoblasts from mice of the indicated genotypes were differentiated in myogenic medium for 5 days. Representative micrographs are shown (n = 3 independent experiments). Scale bars: 100 μm.

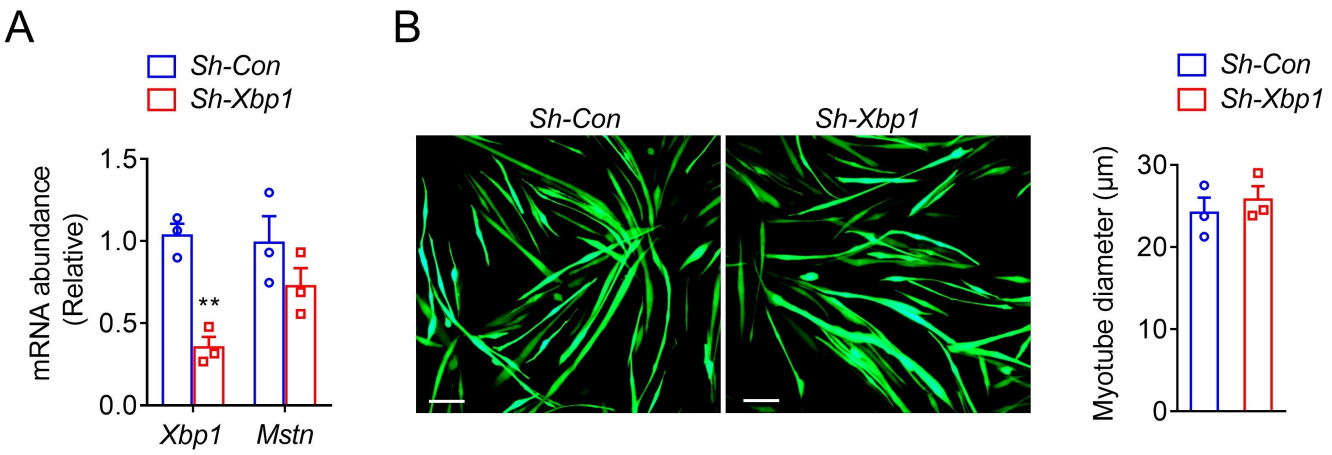

Supplemental Figure 6. Knockdown of XBP1 expression does not affect myotube hypertrophy. (A) Quantitative RT-PCR analysis of Xbp1 and Mstn mRNA abundance in C2C12 myotubes infected for 48 hours with Sh-Con or with Sh-Xbp1 adenovirus expressing a shRNA directed against XBP1 (n = 3 independent experiments). **(B)** C2C12 myoblasts were infected with EGFP-expressing adenovirus and then differentiated for 4 days, followed by infection with Sh-Con or Sh-Xbp1 adenovirus for 2 days. Representative images of myotubes by fluorescence microscopy (n = 3 independent experiments). Scale bars: 100 μm. Quantification of myotube diameters is shown. All data are shown as the mean ± SEM. $^{**}P<0.01$ by two-tailed unpaired Student's t-test.

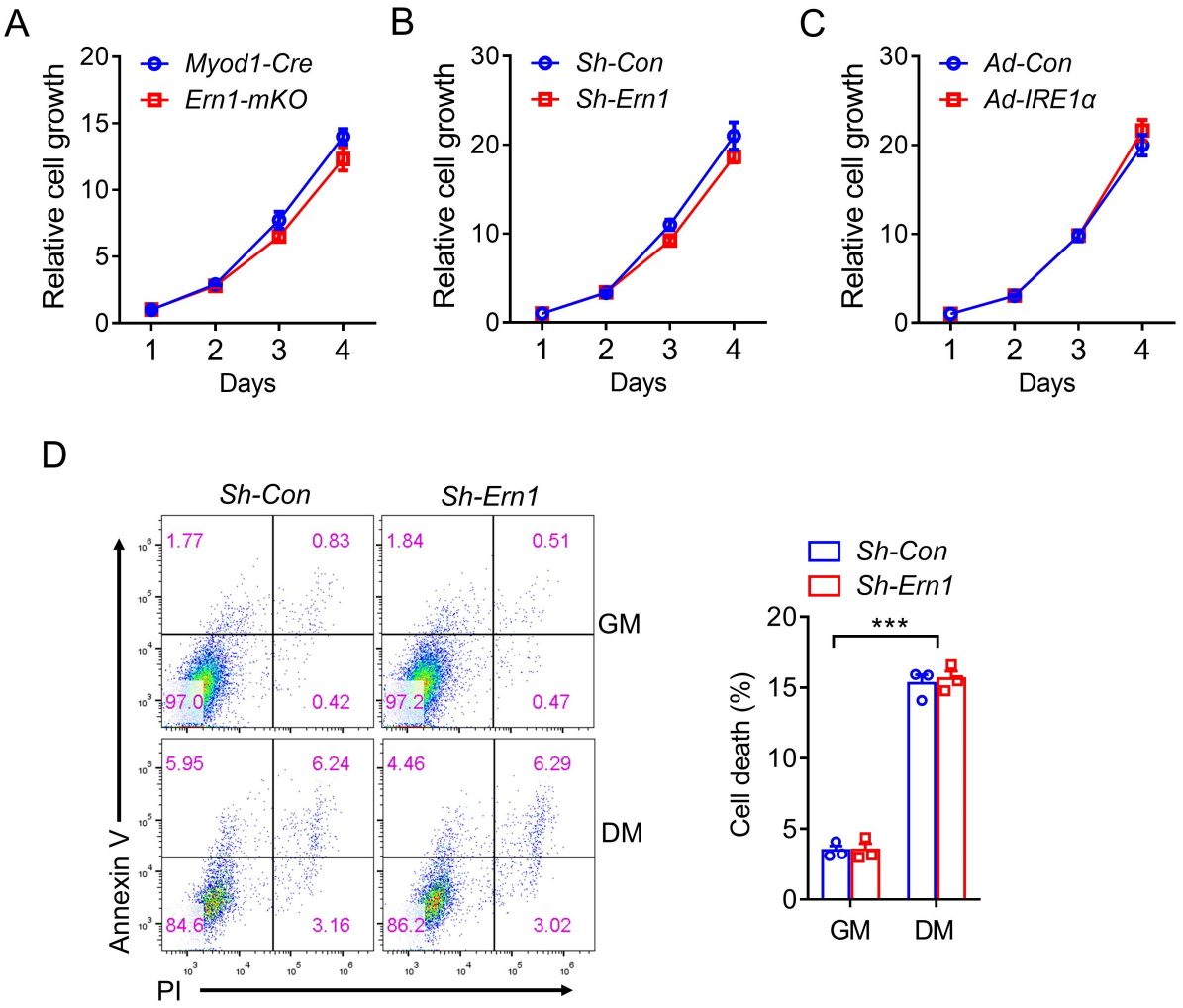

Supplemental Figure 7. IRE1α does not affect the proliferation or cell death of myoblasts. (A) MTT analysis of the proliferation rate of primary myoblasts isolated from *Myod1-Cre* and *Ern1*$^{f/f}$*;Myod1-Cre* (Ern1-mKO) mice (n = 3 independent experiments). **(B-C)** MTT analysis of the proliferation rate of C2C12 cells infected for 24 hours with **(B)** adenoviruses expressing scramble control shRNA (Sh-Con) or shRNA directed against IRE1α (Sh-Ern1), or **(C)** control adenovirus (Ad-Con) or human IRE1α-expressing adenovirus (Ad-IRE1α) (n = 3 independent experiments). **(D)** C2C12 cells infected for 24 hours with Sh-Con or Sh-Ern1 adenoviruses were incubated in GM (Growth Medium) or DM (Differentiation Medium) for 24 hours. Cells were collected and stained for Annexin V and propidium iodide (PI), and then analyzed by FACS for cell death analysis. Representative FACS plots are shown, and percentages of dead cells (Annexin V$^+$ plus PI$^+$) are quantified (n = 3 independent experiments). All data are shown as the mean ± SEM. $^{***}P < 0.001$ by 2-way ANOVA with Bonferroni's multiple comparisons test.

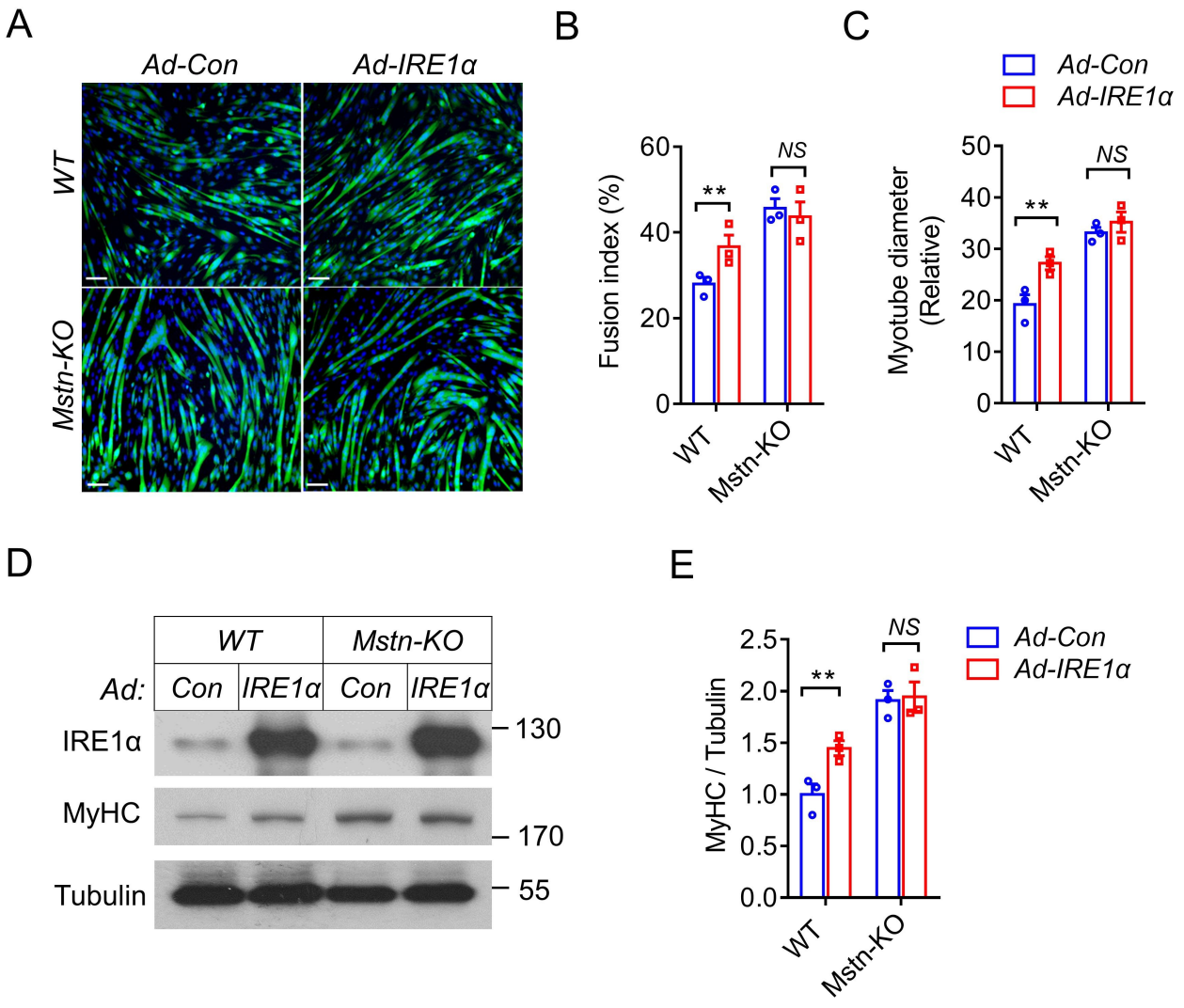

Supplemental Figure 8. Myostatin mediates IRE1α's regulatory effect upon muscle cell differentiation and growth. Wild-type (WT) and Mstn-KO C2C12 myoblast cells were infected for 24 hours with empty control adenovirus or that expressing human IRE1α before differentiation for 2 days in myogenic medium. **(A)** Representative images of MyHC immunostaining (n = 3 independent experiments). Scale bars: 100 μm. **(B, C)** Quantification of the fusion index **(B)** and myotube diameters **(C)** (n = 3 independent experiments). **(D, E)** Immunoblot analysis of the indicated proteins **(D)**, and quantification of averaged MyHC/Tubulin levels **(E)** (n = 3 independent experiments). All results represent the mean ± SEM. $^{**}P<0.01$ by 2-way ANOVA with Bonferroni's multiple comparisons test. NS, no significance.

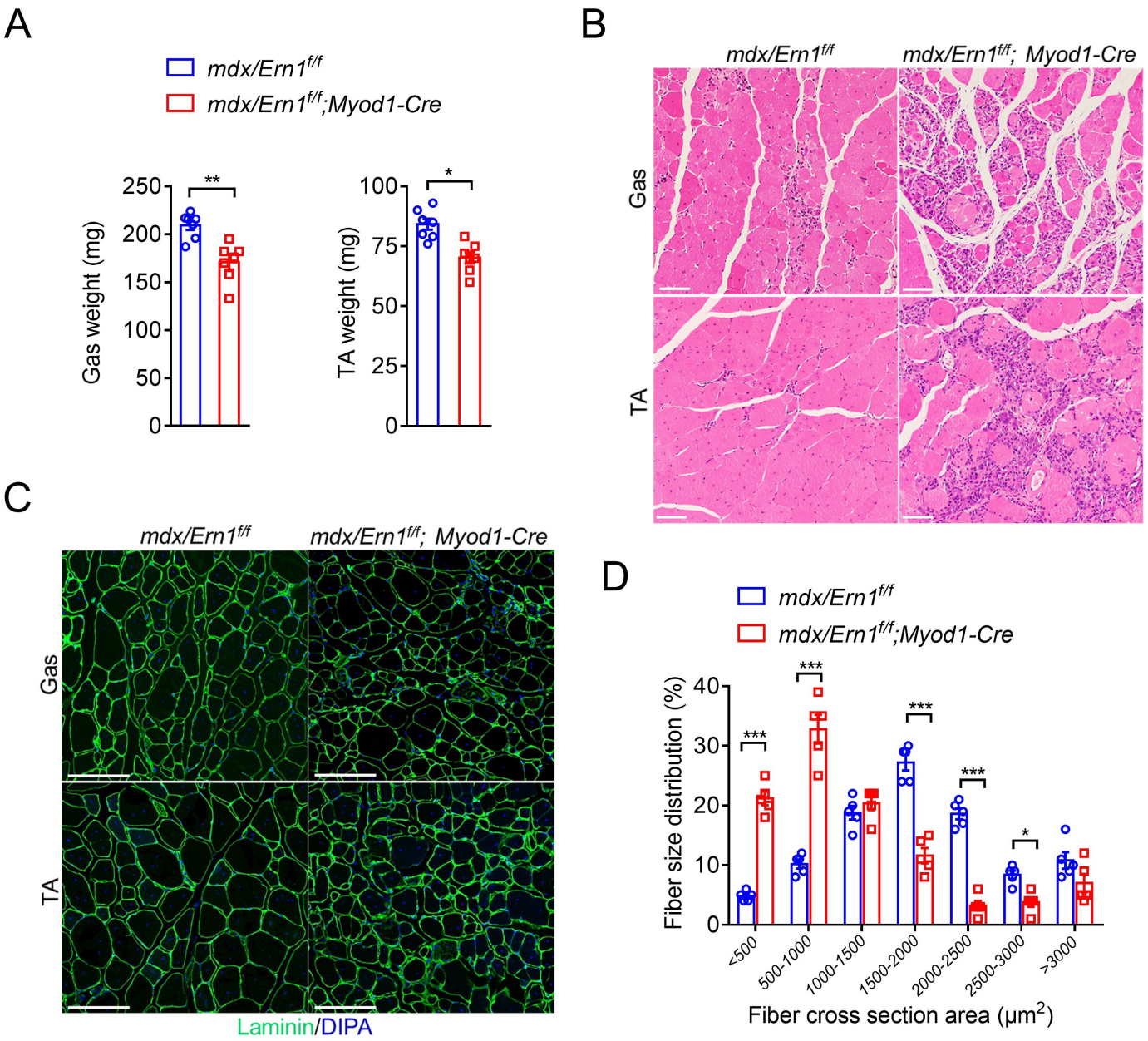

Supplemental Figure 9. IRE1α abrogation worsens the dystrophic phenotypes in older *mdx* mice. (A) The weight of gastrocnemius (Gas) and TA muscles from male *mdx/Ern1$^{f/f}$* and *mdx/Ern1$^{f/f}$;Myod1-Cre* mice at 21 weeks of age (n = 7 mice per genotype). Representative images of H&E staining **(B)** and Laminin (green) immunostaining **(C)** of Gas and TA muscles (n = 5 mice per genotype). Scale bars: 100 μm. **(D)** Percentage of myofibers in the indicated cross-sectional areas of TA muscle. Quantification was conducted by ImageJ from 500 myofibers of the TA muscle from each mouse (n = 5 mice per genotype). Data are shown as the mean ± SEM. $^{*}P<0.05$, $^{***}P<0.001$ by two-tailed unpaired Student's t-test **(A)** or 2-way ANOVA **(D)** with Bonferroni's multiple comparisons test.

Table S1: Sequence of oligonucleotide primers used for RT-PCR analysis.

Oligonucleotide primer pairs list	
Myogenin-F	5'- ACCTTCAGGGCTTCGAGCC -3'
Myogenin-R	5'-AAGGGAGTGCAGATTGTGGGC-3'
Myh1-F	5'- TAAACGCAAGTGCCATTCCTG -3'
Myh1-R	5'- GGGTCCGGGTAATAAGCTGG -3'
Myh2-F	5'- GAGTAGCTCTTGTGCTACCCAGC -3'
Myh2-R	5'- AATTGCTTTATTCTGCTTCCACC -3'
Myh4-F	5'- CTTTGCTTACGTCAGTCAAGGT -3'
Mhy4-R	5'- AGCGCCTGTGAGCTTGTAAA -3'
18s-F	5'- AGGGGAGAGCGGGTAAGAGA -3'
18s-R	5'- GGACAGGACTAGGCGGAACA -3'
Mstn-F	5'-AATCCCGGTGCTGCCGCTACCCCCTCA -3'
Mstn-R	5'- GAGCCTCTGGGGTTTGCTT-3'
MyoPPT-F	5'-AGTGGATCTAAATGAGGGCAGT-3'
MyoPPT-R	5'-GTTTCCAGGCGCAGCTTAC-3'
Gapdh-F	5'- TGGAAAGCTGTGGCGTGAT -3'
Gapdh-R	5'- TGCTTCACCACCTTCTTGAT -3'
Blos1-F	5'- TCCCGCCTGCTCAAAGAAC-3'
Blos1-R	5'- GAGGTGATCCACCAACGCTT-3'
Chop-F	5'- CCT AGC TTG GCT GAC AGA GG-3'
Chop-R	5'- CTG CTC CTT CTC CTT CAT GC-3'
Atf4-F	5'- CTCCTCTTCGCACTTCTGCTC -3'
Atf4-R	5'- CCTTCGACCAGTCGGGTTTG-3'
Xbp1t-F	5'- AAGAACACGCTTGGGAATGG -3'
Xbp1t-R	5'- ACTCCCCTTGGCCTCCAC -3'
Xbp1s-F	5'- GAGTCCGCAGCAGGTG -3'
Xbp1s-R	5'- GTGTCAGAGTCCATGGGA -3'
Igf1-F	5'- CTGGACCAGAGACCCTTTGC -3'
Igf1-R	5'- GGACGGGGACTTCTGAGTCTT -3'

Supplemental Methods

CTX-induced skeletal muscle injury. CTX-induced acute skeletal muscle degeneration was performed as described previously (1). Briefly, CTX from *Naja atra* (Shanghai Boyao Biological Technology) was dissolved in sterile saline to a final concentration of 1 mg/ml. After anesthetization with isoflurane, mouse legs were shaved and cleaned with alcohol. TA muscles were injected with 50 μl of CTX with a 26-gauge needle.

Histologic analyses. Immediately after sacrifice, skeletal muscles were removed from mice and fixed in 10% neutral formalin for 48 h at 4 °C. Muscle tissues were embedded in paraffin and cut to 5-μm sections on slides. Muscle sections were then stained with hematoxylin and eosin (MilliporeSigma) according to the standard protocol. Immunofluorescent staining of laminin and eMyHC was performed using Laminin antibody (catalog Ab11576, Abcam) and eMyHC (catalog sc-53097, Santa Cruz Biotechnology Inc.) antibody as previously described (2). Quantification of cross-sectional area of the myofibers was performed in a blinded manner using the NIH ImageJ software.

Endurance exercise studies. Mice were acclimated (running for 9 min at 10 m/min followed by 1 min at 20 m/min) to the treadmill for 2 consecutive days prior to exercise experiments. Endurance exercise was performed as described previously (3). Briefly, *ad libitum* fed mice were allowed to run for 10 min at 10 m/min followed by a constant speed of 18 m/min until exhaustion.

Evans blue staining. Evans blue dye (1% solution, MilliporeSigma) was injected intraperitoneally at a concentration of 0.01 ml volume per gram of body weight. After 24 h, mice were sacrificed, and skeletal muscles were frozen for preparation of histological sections. Evans blue incorporation was analyzed by fluorescence microscopy.

Serum creatine kinase assay. Mouse blood was collected and serum was prepared using microhematocrit tubes (Fisher Scientific). Serum creatine kinase activity was determined in a blinded fashion using a Creatine Kinase Assay Kit (catalog OSR61155, Beckman Coulter) according to the manufacturer's instructions.

AAV2/9-MyoPPT inhibition of Myostatin in vivo. To generate the recombinant adeno-associated virus 2/9 (AAV2/9) expressing the N-terminal propeptide (MyoPPT, amino acid 1-267) of mouse Myostatin (4, 5), PCR was performed using the primers: 5'-TTTGGCAAAGAATTGGATCCGCCACCATGATGCAAAAACTGCAAATGT ATG-3' and 5'-GGTTGATTATCGATAAGCTTTCATCTCCGGGACCTCTTGGGTGTG-3'. The PCR products were then subcloned into an pAAV-CAG plasmid to produce the pAAV-CAG-MyoPPT plasmid. AAVs were subsequently generated using packaging plasmids pAAV-helper and pAAV2/9 together with pAAV-CAG-MyoPPT or pAAV-CAG-GFP by ChuangRui Bio. Viruses were administered by intraperitoneal injection at a dose of $3x10^{11}$ vg per mouse at postnatal day 3 (P3) and day 6 (P6).

Cell culture and adenovirus infection. Primary myoblasts were isolated from TA muscles of *Myod1-Cre* and *Ern1$^{f/f}$;Myod1-Cre* mice as described (6). Briefly, mice

were sacrificed via CO_2 inhalation followed by cervical dislocation. TA muscles were collected, minced, and digested with an enzyme solution (0.75 U/ml Collagenase D, 1 U/ml dispase type II and 2.5 mM $CaCl_2$) for 1 h at 37 °C in a shaking bath. Pre-plate medium (PPM), i.e. Dulbecco's Modified Eagle's Medium (DMEM) (Invitrogen) supplemented with 10% fetal bovine serum (HyClone, Thermo Scientific), was added and samples were triturated gently before loading onto a Netwell filter (70 μm, BD). Cells were pelleted by centrifugation, re-suspended in PPM, and plated on an uncoated plate for 2 h at 37°C. Non-adherent cells were collected by centrifugation and the pellet was re-suspended in a growth medium (HAM's F-10 medium, 20% FBS and 5 ng/ml bFGF; Invitrogen and MilliporeSigma). Myoblasts were cultured for expansion on plates coated with rat tail veil collagen II (Invitrogen), and fed daily with the growth medium. For differentiation, cells were washed with PBS and cultured in the DMEM medium (Gibco, Invitrogen) containing 2% horse serum and re-fed daily with this differentiation medium.

C2C12 cells was obtained from the American Type Culture Collection. WT and *Mstn*-KO C2C12 cells were generated as previously described (7). Cells were cultured at 37°C with 5% CO_2 in DMEM (Invitrogen) supplemented with 10% FBS (HyClone, Thermo Scientific, USA) and 1% penicillin/streptomycin (P/S) (Gibco, Invitrogen). For differentiation, C2C12 cells were cultured in DMEM differentiation medium (Gibco, Invitrogen) with 2% horse-serum. Recombinant adenoviruses for overexpressing control, human IRE1α and its mutant forms and XBP1s, as well as Sh-Con scramble control, Sh-Ern1 or Sh-Xbp1, were prepared and used as described

previously (8-10). Myoblasts or differentiated myotubes were infected with adenoviruses as indicated at a MOI of 100 overnight before further manipulations for differentiation or harvesting for analysis at 48 h post-infection.

Flow-cytometry analysis of muscle satellite cells. MuSCs were isolated and analyzed based on previously reported method (11). Briefly, TA muscles were collected, minced, and digested with an enzyme solution (0.75 U/ml Collagenase D, 1 U/ml dispase type II and 2.5 mM $CaCl_2$) for 1.5 h at 37 °C in a shaking bath. Digested muscles were then triturated and washed in Hams F-10 medium (Gibco, Invitrogen) containing 10% FBS and 1% penicillin/streptomycin. Mononuclear cells were filtered with a 45-mm cell strainer and stained with the antibody mix including Vcam1-APC, CD31-FITC, CD45-FITC and Sca1-FITC (catalog 17106182, 11031185, 11045182 11598182, eBioscience) along with PI (MilliporeSigma). All antibodies were used at a dilution of 1:100. Cells were analyzed using the CyAn ADP High-Performance Flow Cytometer (Beckman Coulter), and cells with $Sca1^-/CD31^-/CD45^-/VCAM1^+$ signals were considered as representing the population of MuSCs.

Immunohistochemistry. Myocytes were fixed with 4% paraformaldehyde for 15 min, and blocked for 1 h with blocking buffer (5% goat serum, 3% BSA, 0.3% triton X-100 in PBS). Cells were incubated with MyHC antibody (MF20, catalog AB2147781; Developmental Studies Hybridoma Bank, 1:200) overnight at 4°C, followed by incubation with secondary antibodies conjugated with AlexaFlour-488 fluorescent dyes (catalog A21141, Thermo Fisher Scientific, 1:400) for 1 h at room temperature. Nuclei were stained by DAPI (catalog D-9542, MilliporeSigma,

1:10000). Images were acquired by fluorescent microscopy. The fusion index was calculated as the ratio of the number of nuclei incorporated into myotubes (> 2 nuclei) to the total number of nuclei. Nuclei were counted from five images per group using NIH ImageJ software. Multinuclear myotube formation was assessed by calculating the percentage of nuclei incorporated into the MyHC positive myotubes relative to total number of cells.

Antibodies and immunoblot analyses. The antibody directed against phosphorylated IRE1α at Ser^{724} (p-IRE1α) (catalog NB100-2323) was purchased from Novus Biologicals, and the antibodies against MyHC (MF20, catalog AB2147781) and eMyHC (catalog sc-53097) were from Developmental Studies Hybridoma Bank and Santa Cruz Biotechnology Inc., respectively. Antibodies against Hsp90 (catalog 4877), IRE1α (catalog 3294), eIF2α (catalog 5324), p-eIF2α (catalog 3398), BiP (catalog 3177), S6K (catalog 2708), p-S6K (catalog 9204), Smad3 (catalog 9513) and p-Smad3 (catalog 13120) were all from Cell Signaling Technology. Anti-α-tubulin antibody (catalog T6199) was from MilliporeSigma. Anti-myostatin antibody (catalog ab201954) was from Abcam. Total protein was extracted from cultured cells or tissues using RIPA buffer (150 mM NaCl, 1% NP-40, 0.5% sodium deoxycholate, 0.1% SDS and 50 mM Tris-HCl, pH 7.4) containing complete protease-inhibitor cocktail (MilliporeSigma). Protein concentrations were measured by Bradford Protein Assay Kit (catalog 23200, Thermo Scientific). Western immunoblotting was performed as previously described (10), and quantification of the immunoblots was done using the NIH ImageJ software.

Quantitative RT-PCR analyses. Total RNA was extracted from mouse muscle samples or C2C12 cells using TRIzol reagent (Invitrogen). Isolated RNA integrity was verified by electrophoresis with ethidium bromide staining. One μg total RNA was used for cDNA synthesis with the M-MLV reverse transcriptase (Invitrogen) and random hexamer primers according to the manufacturer's instructions. Real-time quantitative PCR was then performed using the ABI Step-one Plus system (Applied Biosystems) with SYBR Green PCR reagents (Applied Biosystems). Oligonucleotide primers for the target genes analyzed are listed in Table S1. Normalization was done using 18s rRNA or *Gapdh* as the internal control.

IRE1α and Myostatin expression plasmids. Expression constructs for the Flag-tagged full-length or deletion mutant human IRE1α were generated as previously described (8). For Myostatin overexpression, the full coding region of mouse *Mstn* was amplified by RT-PCR from C2C12 cells using the following primer pair, 5'-TAGCGCTACCGGACTCAGATATGATGCAAAAAATGTATGTTTATATTTA CCT-3' and 5'-AATCAGCTCGCTCATGACCGGTGAGCACCCACAGCGGTCTAC-3'. The PCR products were then subcloned into the Plvx-puro vector. Plasmids for the expression of the GC-to-CA and the 14-nucleotide stem-loop deletion (ΔSL) mutant *Mstn* were generated with the Q5® High-Fidelity DNA Polymerase (BioLabs) and MultiF Seamless Assembly Mix (catalog RK21020, Abclonal) using the following primer pairs, respectively: 5'-CAGCTCCTAACATCACAAAAGATGCTATAAGACAACTTC-3' and

5’-AGAAGTTGTCTTATAGCATCTTTTGTGATGTTAGGAGCTG-3’; and 5’-GCTCCTAACTATAAGACAACTTCTGCCAAGAGCGCCTCC-3’ and 5’-TCTTATAGTTAGGAGCTGTTTCCAGGCGCAGC-3’.

RNA-binding protein immunoprecipitation (RIP) assay. RIP assay was performed using the Magna RIP^{TM} kit according to the Manufacturer’s protocol (MilliporeSigma). Briefly, HEK293T cells were obtained from the American Type Culture Collection and were cultured at 37°C with 5% CO_2 in DMEM (Invitrogen) supplemented with 10% FBS (HyClone, Thermo Scientific, USA) and 1% penicillin/streptomycin (P/S) (Gibco, Invitrogen). HEK293T cells were co-transfected for 24 h with plasmids expressing the wild-type (wt) or stem-loop deletion (ΔSL) mutant Myostatin, together with vector control or plasmids expressing Flag-tagged human WT or deletion mutant IRE1α proteins. Total cell lysates were incubated with excess anti-Flag (catalog 14793, Cell Signaling Technology) antibody at 4°C overnight followed by incubation with protein A/G magnetic beads and centrifugation. Precipitated IRE1α/RNA complexes were treated with RNase-free DNase and proteinase K to remove trapped genomic DNAs and proteins, and RNA was further extracted with TRIzol reagent and subjected to RT-PCR analysis using the following *Mstn* primer pair, 5’-AGTGGATCTAAATGAGGGCAGT-3’ and 5’-GTTTCCAGGCGCAGCTTAC-3’.

Myostatin mRNA decay analysis. For analysis of the stability of *Mstn* mRNA, the RNA polymerase II inhibitor, actinomycin D (catalog A1410, MilliporeSigma) (5 μg/ml), was added to differentiated C2C12 myotubes infected for 48 hours with

Sh-Con or Sh-Ern1 adenoviruses, or with Ad-Con or Ad-IRE1α adenoviruses. Total RNA was isolated at the desired incubation time intervals before analysis by quantitative RT-PCR. The abundance of *Mstn* mRNA was determined using *Gapdh* mRNA as an internal control.

Myostatin ELISA assay. Myostatin protein from cell culture medium or serum of mice was measured by ELISA kit (catalog DGDF80, R&D system) according to Manufacturer's instructions.

Cell proliferation/viability and cell death analyses. Similar number of myoblasts was seeded in 96-well plates, and cell viability was measured daily by MTT assay for 4 days. Briefly, 20 μl of MTT (catalog ab211091, Abcam) working solution (5 mg/ml) was added to each well, followed by incubation at 37°C for 3 h. The supernatants were then removed, and the resultant MTT formazan was dissolved in 100 μl of DMSO. The absorbance was measured at the wavelength of 590 nm. Cell death analysis was performed using Annexin V/propidium iodide (PI) (catalog 13241 Invitrogen) staining followed by FACS analysis. Briefly, C2C12 myoblasts were cultured in 12-well plates and differentiated. Cells were then collected and washed before staining with FITC-annexin V and PI, followed by FACS analysis on the CyAn ADP Flow Cytometer (Beckman Coulter). Data were analyzed with the FlowJo Software.

In vitro assay of IRE1α-catalyzed mRNA cleavage. Fluorescence-based in vitro biochemical analysis of IRE1α-catalyzed cleavage of mRNA encoding Myostatin was designed as previously described (12). An RNA molecule with the 14-nucleotide

sequence (WT, 5'-CAUCAGCAAAGAUG-3'; Mut, 5'-CAUCACAAAAGAUG-3') corresponding to the putative RIDD region of *Mstn* mRNA was synthesized (Takara), which harbors FAM and BQH1 at its 5'- and 3'-end, respectively, for fluorescent quenching. This synthetic *Mstn* RNA at 50 nM in 10 μl reaction buffer (50 mM HEPES, 100mM KOAc, 0.005% Triton, 1mM DTT, pH7.2) was mixed and incubated with recombinant human IRE1α protein at 6 nM in the presence of DMSO or 10 μM 4μ8C in 10 μl reaction buffer for 1 h at room temperature. Fluorescence intensity was measured using a Cytation3 plate reader (excitation 485 nm, emission 535 nm).

References

1. Yan Z, Choi S, Liu X, Zhang M, Schageman JJ, Lee SY, Hart R, Lin L, Thurmond FA, and Williams RS. Highly coordinated gene regulation in mouse skeletal muscle regeneration. *The Journal of biological chemistry.* 2003;278(10):8826-36.
2. Xiong G, Hindi SM, Mann AK, Gallot YS, Bohnert KR, Cavener DR, Whittemore SR, and Kumar A. The PERK arm of the unfolded protein response regulates satellite cell-mediated skeletal muscle regeneration. *eLife.* 2017;6:e22871
3. Liu J, Liang X, Zhou D, Lai L, Xiao L, Liu L, Fu T, Kong Y, Zhou Q, Vega RB, et al. Coupling of mitochondrial function and skeletal muscle fiber type by a miR-499/Fnip1/AMPK circuit. *EMBO molecular medicine.* 2016;8(10):1212-28.
4. Qiao C, Li J, Jiang J, Zhu X, Wang B, Li J, and Xiao X. Myostatin propeptide gene delivery by adeno-associated virus serotype 8 vectors enhances muscle growth and ameliorates dystrophic phenotypes in mdx mice. *Human gene therapy.* 2008;19(3):241-54.
5. Mouisel E, Relizani K, Mille-Hamard L, Denis R, Hourde C, Agbulut O, Patel K, Arandel L, Morales-Gonzalez S, Vignaud A, et al. Myostatin is a key mediator between energy metabolism and endurance capacity of skeletal muscle. *American journal of physiology Regulatory, integrative and comparative physiology.* 2014;307(4):R444-54.
6. Rando TA, and Blau HM. Primary mouse myoblast purification, characterization, and transplantation for cell-mediated gene therapy. *The Journal of cell biology.* 1994;125(6):1275-87.

7. Wang L, Huang Y, Wang X, and Chen Y. Label-Free LC-MS/MS Proteomics Analyses Reveal Proteomic Changes Accompanying MSTN KO in C2C12 Cells. *BioMed research international.* 2019;2019:7052456.

8. Qiu Y, Mao T, Zhang Y, Shao M, You J, Ding Q, Chen Y, Wu D, Xie D, Lin X, et al. A crucial role for RACK1 in the regulation of glucose-stimulated IRE1alpha activation in pancreatic beta cells. *Science signaling.* 2010;3(106):ra7.

9. Mao T, Shao M, Qiu Y, Huang J, Zhang Y, Song B, Wang Q, Jiang L, Liu Y, Han JD, et al. PKA phosphorylation couples hepatic inositol-requiring enzyme 1alpha to glucagon signaling in glucose metabolism. *Proceedings of the National Academy of Sciences of the United States of America.* 2011;108(38):15852-7.

10. Shao M, Shan B, Liu Y, Deng Y, Yan C, Wu Y, Mao T, Qiu Y, Zhou Y, Jiang S, et al. Hepatic IRE1alpha regulates fasting-induced metabolic adaptive programs through the XBP1s-PPARalpha axis signalling. *Nature communications.* 2014;5:3528.

11. Liu L, Cheung TH, Charville GW, and Rando TA. Isolation of skeletal muscle stem cells by fluorescence-activated cell sorting. *Nature protocols.* 2015;10(10):1612-24.

12. Wiseman RL, Zhang Y, Lee KP, Harding HP, Haynes CM, Price J, Sicheri F, and Ron D. Flavonol activation defines an unanticipated ligand-binding site in the kinase-RNase domain of IRE1. *Molecular cell.* 2010;38(2):291-304.